Table 2.4 Ford–Philips 4-215 engine Ideal Isothermal simulation.

Engine and Operating parameters	
Clearance volumes	$V_{clc} = V_{cle} = 214.2$ cc
Swept volumes	$V_{swc} = V_{swe} = 870.6$ cc
Void volumes: Cooler	$V_k = 164.3$ cc
Regenerator	$V_r = 705.8$ cc
Heater	$V_h = 510.9$ cc
Mean pressure	$p_{mean} = 150$ bar
Mass of gas in engine	$M = 16.2$ g
Hot space temperature	$T_h = 1023$ K
Cold space temperature	$T_k = 337$ K
Ideal Isothermal performance	
Work done	$W = 3870.3$ J/cycle
Heat transferred to gas in hot space	$Q_e = 5771.6$ J/cycle
Heat transferred to gas in cold space	$Q_c = -1901.3$ J/cycle
Thermal efficiency	$\eta = W/Q_e = 67.1\%$
Indicated power output	Power = 212.9 kW at 3300 rpm

Note. The engine is considered as having a single cycle.
All volumes per cylinder are multiplied by four.

The pressure/volume indicator diagram shown in figure 2.7 is the standard means of characterising an engine. The engine size is indicated by the total volume variation and its mass by the maximum pressure, the work done being equal to the area enclosed by the curve.

2.5 Case study—The General Motors GPU-3 engine

2.5.1 The rhombic drive mechanism

The rhombic drive mechanism was invented by R J Meijer of Philips in 1959 (Meijer 1959), and is shown schematically in figure 2.8. The system consists of separate displacer and power pistons which have conveniently separated functions. The displacer separates the hot and cold spaces at approximately the same pressure and is used to shuttle the working gas between these spaces. The power piston provides both the compression and the expansion processes. There are two cranks which are geared together so as to counter-rotate and drive the yokes, to which are attached the displacer and power piston rods. A pressurised buffer space allows the engine to operate at high mean pressures without requiring a pressurised crankcase. Thus only two shaft seals are required on the displacer and power piston rods.

The success of this arrangement is due to the fact that the two pistons have no side forces, as the horizontal components of the forces exerted by each pair

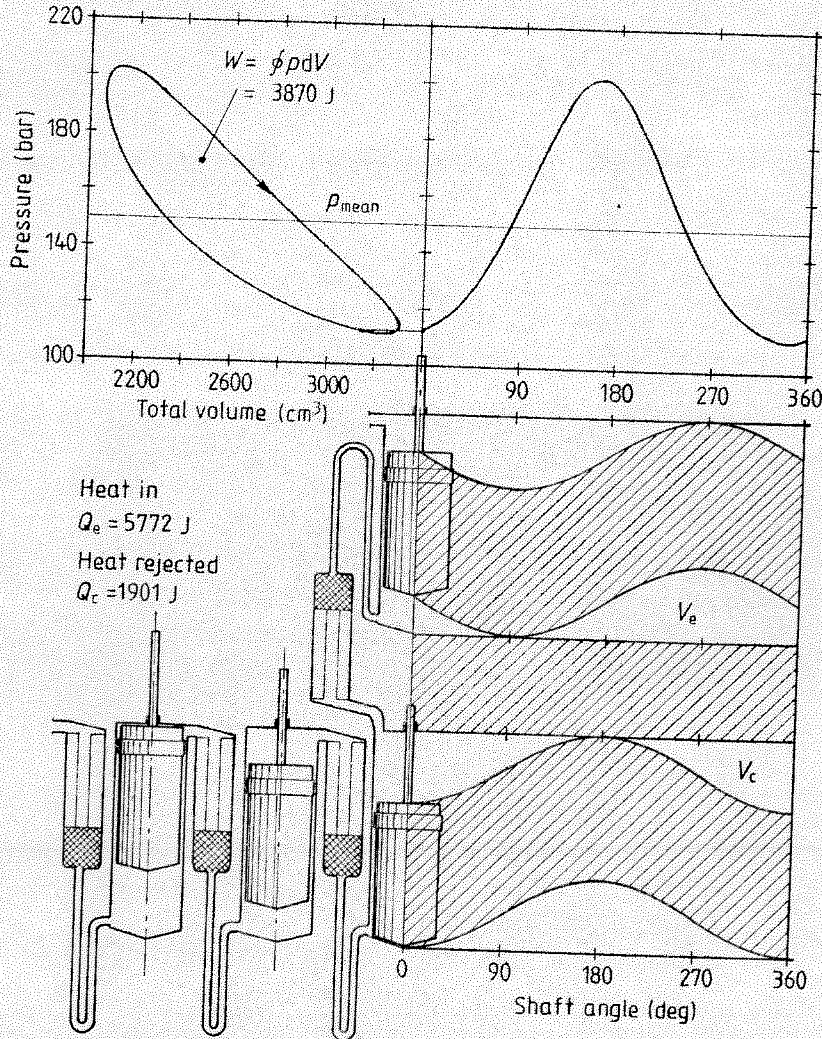

Figure 2.7 Ford–Philips 4-215 engine—Ideal Isothermal simulation.

of connecting rods are exactly balanced at each yoke. Furthermore, complete static and dynamic balancing is attainable in the single cylinder arrangement, allowing vibrationless high-speed operation. The principle disadvantage of the rhombic drive engine is its relative complexity.

The rhombic drive mechanism does not produce sinusoidal volume variations. The actual volume variations are functions of the various geometric parameters of the mechanism and are derived from geometrical considerations, as in figure 2.9. The complete set of equations is summarised in figure 2.10, in which the working space volumes and volume derivatives are shown as functions of the crank angle θ. The initial condition ($\theta = 0$) has been arbitrarily chosen as the point of maximum compression space volume.

2.5.2 The GPU-3 engine

The GPU-3 (Ground Power Unit) is a rhombic drive Stirling engine generator set which was developed by the General Motors Research

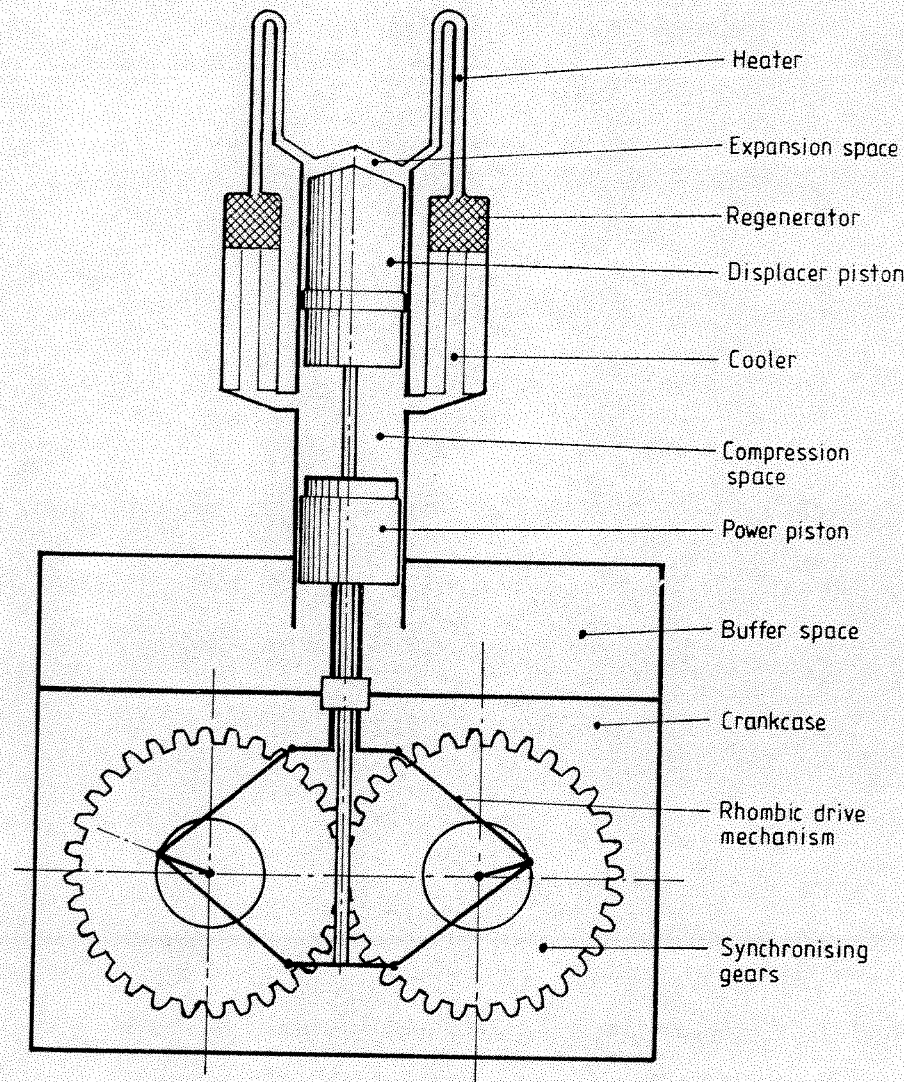

Figure 2.8 Rhombic drive engine—schematic.

Laboratories for the US Army in 1965. The engine is capable of producing a maximum brake output of 7.5 kW using hydrogen as the working fluid pressurised to 69 bar.

Only a few experimental units were actually built by GM. NASA Lewis Research Center has recently restored one unit to operating condition, which is being tested as part of a Stirling engine technology study for the US Department of Energy (Cairelli *et al* 1978). A general view of the GPU-3 is shown in figure 2.11 and a cross section view is shown in figure 2.12.

The rhombic drive engine of the GPU-3 has been well specified in various NASA Technical Memos, such as that by Tew *et al* (1979), from which table 2.5 has been reproduced. This table gives a complete geometric specification of the GPU-3 engine.

Various baseline tests were run at Lewis Research Center to map the engine performance over a range of heater-tube gas temperatures, mean compression-

Displacement equations

$y_p = r\sin\theta + b_\theta$

$y_d = L_d - b_\theta + r\sin\theta$

where $b_\theta = \sqrt{L^2 - (e + r\cos\theta)^2}$

$y_c = y_d - y_p = L_d - 2b_\theta$

$y_e = y_{dmax} - y_d$

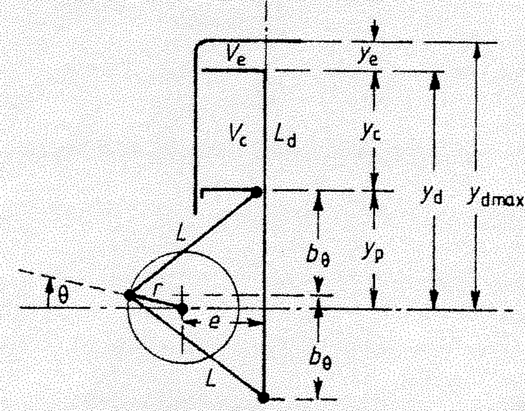

r = crank length
e = eccentricity
L = connecting rod length
L_d = displacer yoke rod length

Compression space

$V_c = V_{clc} + 2A_p(b_1 - b_\theta)$

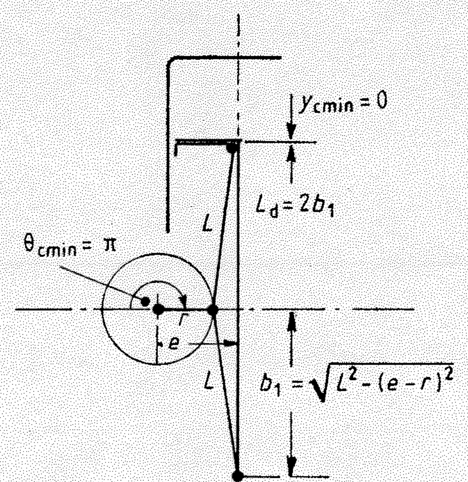

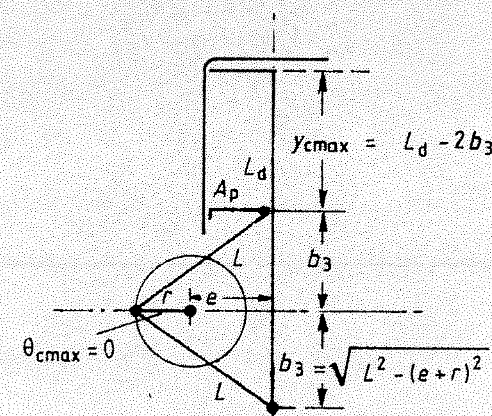

Expansion space

$V_e = V_{cle} + A_d(b_\theta - b_2 - r\sin\theta)$

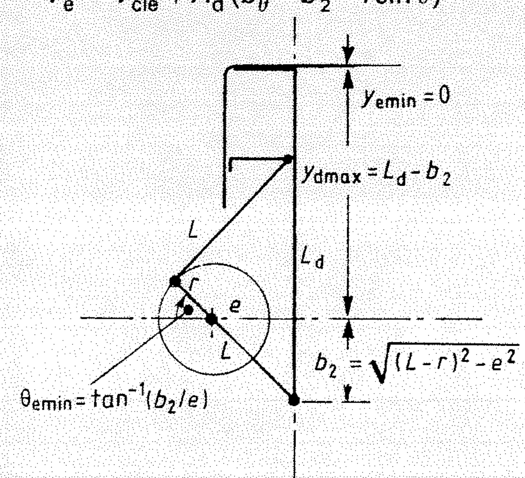

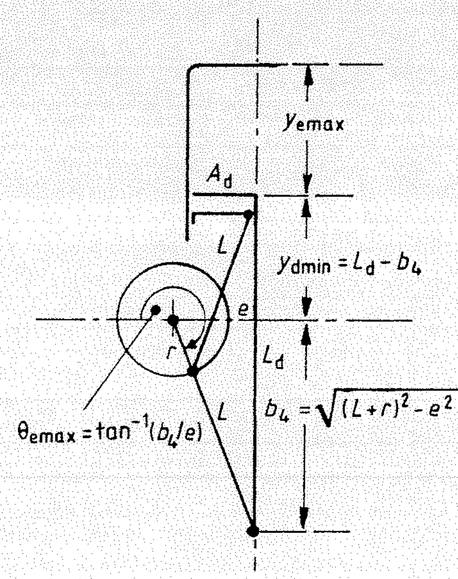

Figure 2.9 Geometric derivation of the rhombic drive equations.

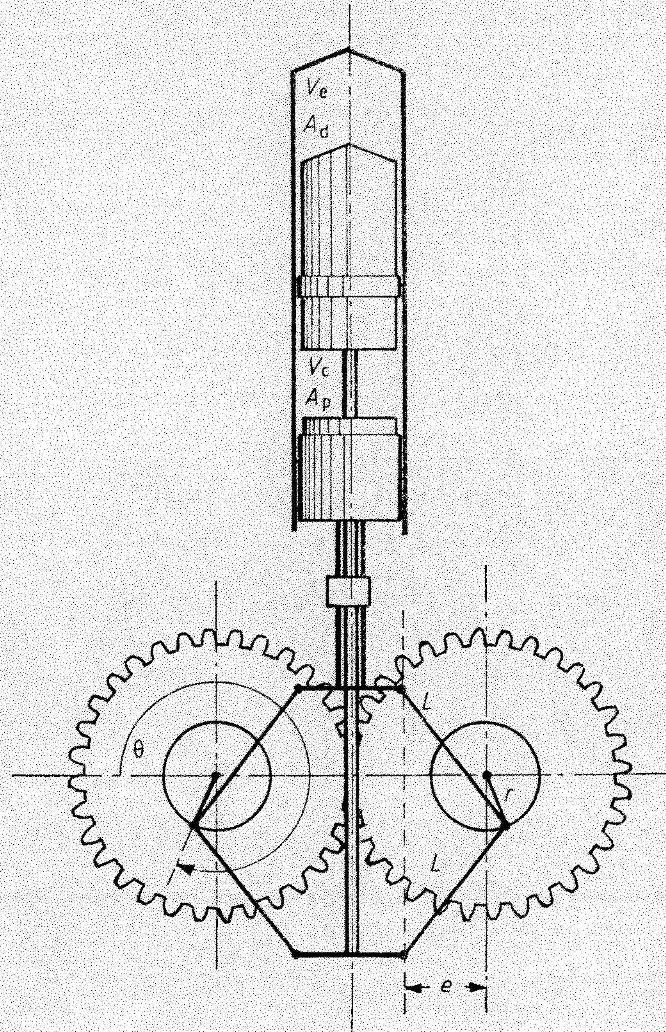

Basic constant parameters

$$b_1 = \sqrt{L^2 - (e-r)^2}$$
$$b_2 = \sqrt{(L-r)^2 - e^2}$$
$$b_3 = \sqrt{L^2 - (e+r)^2}$$
$$b_4 = \sqrt{(L+r)^2 - e^2}$$

Swept volumes

$$V_{swc} = 2A_p(b_1 - b_3)$$
$$V_{swe} = A_d(b_4 - b_2)$$

Volume variations

$$b_\theta = \sqrt{L^2 - (e + r\cos\theta)^2}$$
$$V_c = V_{clc} + 2A_p(b_1 - b_\theta)$$
$$V_e = V_{cle} + A_d(b_\theta - b_2 - r\sin\theta)$$
$$dV_c/d\theta = -2A_p r\sin\theta(e + r\cos\theta)/b_\theta$$
$$dV_e/d\theta = -(dV_c/d\theta)A_d/(2A_p) - A_d r\cos\theta$$

Phase angle advance

$$\alpha \equiv [(\theta_{cmax} - \theta_{emax}) + (\theta_{cmin} - \theta_{emin})]/2$$
$$= \pi - [\tan^{-1}(b_4/e) + \tan^{-1}(b_2/e)]/2$$

Figure 2.10 Rhombic drive engine equation summary.

space pressures, and engine speeds using both helium and hydrogen as the working fluid. These tests were limited to low power levels since the original alternator used was not capable of absorbing the full engine power output. It was decided to simulate the engine under the same conditions as the sample

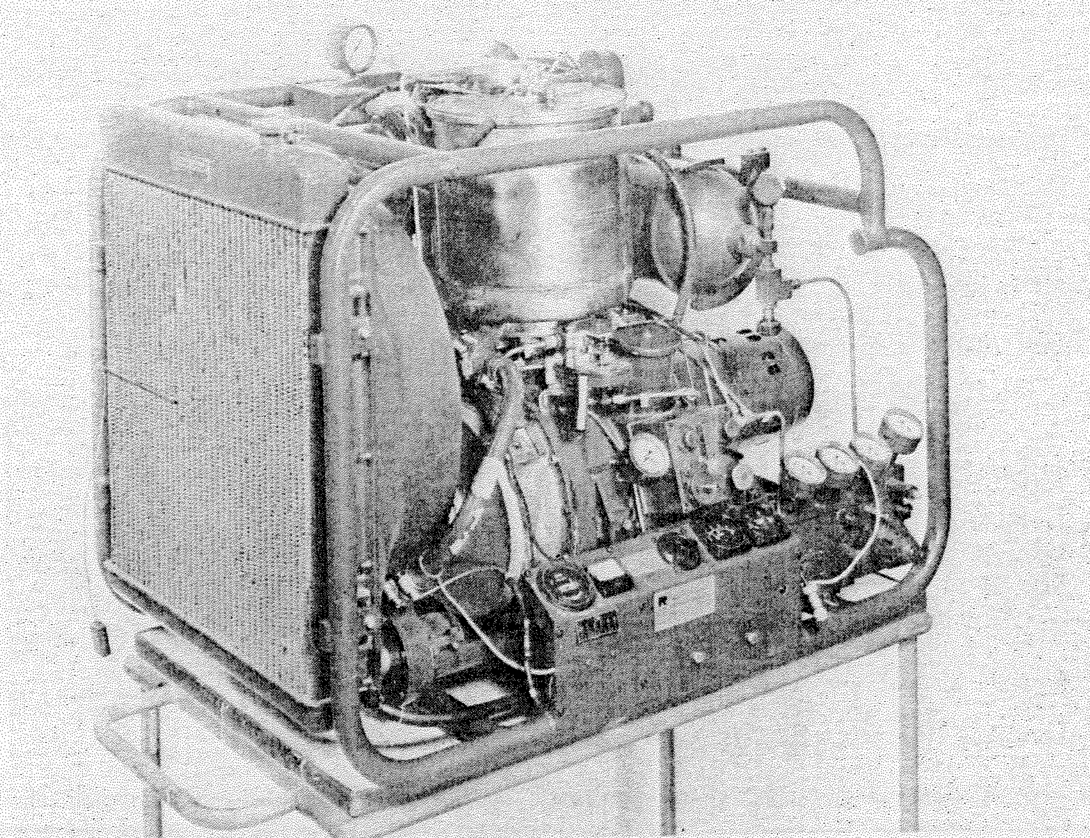

Figure 2.11 The General Motors GPU-3 ground power unit (courtesy NASA Lewis Research Center).

data test point given in Appendix F of the Lewis Research Center report by Thieme (1979). The pertinent operating conditions inferred from the report are summarised as follows:

Working gas:	helium at a mean pressure of 41.3 bar
Operating frequency:	41.72 Hz
Temperatures:	cooler, 288 K; heater, 977 K.

The measured indicated power output was 3958 W at a thermal efficiency of 35%.

The results of simulation using the Ideal Isothermal model are given in table 2.6, and shown diagrammatically in figure 2.13. From the displacement diagram in figure 2.13 we see that the rhombic drive mechanism closely approximates the Ideal Stirling cycle. In particular, the overlapping piston motion allows a large dwell angle during which the compression space volume is almost zero. Thus expansion takes place mainly in the expansion space giving a high specific power output.

The volume variation is highly non-sinusoidal and cannot be described simply. It is difficult even to define the phase angle advance α of the expansion space to compression space volume variations. Measured with respect to the

Table 2.5 GPU-3 engine geometric specification (after Tew *et al* 1979).

GPU 3-2 Engine dimensions and parameters	
Cylinder bore at liner, cm (in)	6.99 (2.751)
Cylinder bore above liner†, cm (in)	7.01 (2.76)
Cooler	
Tube length, cm (in)	4.61 (1.813)
Heat transfer length, cm (in)	3.55 (1.399)
Tube inside diameter, cm (in)	0.108 (0.0425)
Tube outside diameter, cm (in)	0.159 (0.0625)
Number of tubes per cylinder (or number of tubes per regenerator)	312 (39)
Heater	
Mean tube length, cm (in)	24.53 (9.658)
Heat transfer length, cm (in)	15.54 (6.12)
Cylinder tube, cm (in)	11.64 (4.583)
Regenerator tube, cm (in)	12.89 (5.075)
Tube inside diameter, cm (in)	0.302 (0.119)
Tube outside diameter, cm (in)	0.483 (0.19)
Number of tubes per cylinder (or number of tubes per regenerator)	40 (5)
Cold end connecting ducts	
Length, cm (in)	1.59 (0.625)
Duct inside diameter, cm (in)	0.597 (0.235)
Number of ducts per cylinder	8
Cooler end cap, cm^3 (in^3)	0.279 (0.0170)
Regenerators	
Length (inside), cm (in)	2.26 (0.89)
Diameter (inside), cm (in)	2.26 (0.89)
Number per cylinder	8
Material	Stainless steel wire cloth
Number of wires, per cm (per in)	79 × 79 (200 × 200)
Wire diameter, cm (in)	0.004 (0.0016)
Number of layers	308
Filler factor, percent	30.3
Angle of rotation between adjacent screens, deg	5
Drive	
Connecting rod length, cm (in)	4.60 (1.810)
Crank radius, cm (in)	1.38 (0.543)
Eccentricity, cm (in)	2.08 (0.820)
Miscellaneous	
Displacer rod diameter, cm (in)	0.952 (0.375)
Piston rod diameter, cm (in)	2.22(0.875)
Displacer diameter, cm (in)	6.96 (2.740)
Displacer wall thickness, cm (in)	0.159 (0.0625)
Displacer stroke, cm (in)	3.12 (1.23)
Expansion space clearance, cm (in)	0.163 (0.064)
Compression space clearance, cm (in)	0.030 (0.012)
Buffer space maximum volume, cm^3 (in^3)	521 (31.78)
Total working space minimum volume, cm (in)	233.5 (14.25)

†Top of displacer seal is at top of liner at displacer TDC.

Table 2.5 (continued)

GPU-3 Stirling engine dead volumes	
(Volumes are given in cm^3 (in^3))	
I Expansion space clearance volume	
Displacer clearance (around displacer)	3.34 (0.204)
Clearance volume above displacer	7.41 (0.452)
Volume from end of heater tubes into cylinder	1.74 (0.106)
Total	12.5 (0.762)
II Heater dead volume	
Insulated portion of heater tubes next to expansion space	9.68 (0.591)
Heated portion of heater tubes	47.46 (2.896)
Insulated portion of heater tubes next to regenerator	13.29 (0.811)
Additional volume in four heater tubes used for instrumentation	2.74 (0.167)
Volume in header	7.67 (0.468)
Total	80.8 (4.933)
III Regenerator dead volume	
Entrance volume into regenerators	7.36 (0.449)
Volume within matrix and retaining disks	53.4 (3.258)
Volume between regenerators and coolers	2.59 (0.158)
Volume in snap ring grooves at end of coolers	2.18 (0.133)
Total	65.5 (3.998)
IV Cooler dead volume	
Volume in cooler tubes	13.13 (0.801)
V Compression in space clearance volume	
Exit volume from cooler	3.92 (0.239)
Volume in cooler end caps	2.77 (0.169)
Volume in cold end connecting ducts	3.56 (0.217)
Power piston clearance (around power piston)	7.29 (0.445)
Clearance volume between displacer and power piston	1.14 (0.070)
Volume at connections to cooler end caps	2.33 (0.142)
Volume in piston 'notches'	0.06 (0.004)
Volume around rod in bottom of displacer	0.11 (0.007)
Total	21.18 (1.293)
Total dead volume	193.15 (11.787)
Minimum live volume	39.18 (2.391)
Calculated minimum total working space volume	232.3 (14.178)
Measured value of minimum total working space volume (by volume displacement)	233.5 (14.25)
Change in working space volume due to minor engine modification	2.5 (0.15)
	236.0 (14.40)

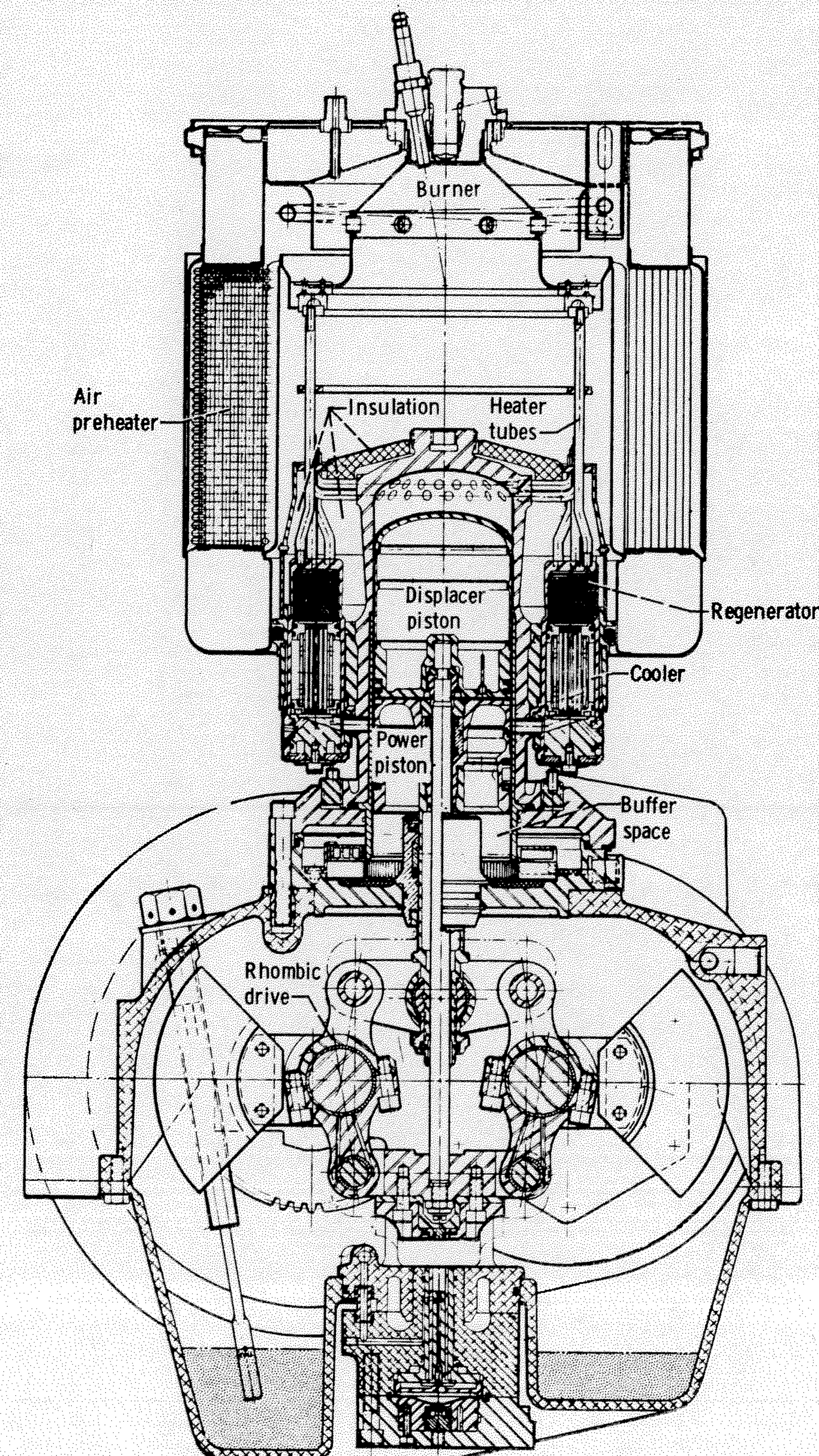

Figure 2.12 Cross section view of the GPU-3 rhombic drive engine (courtesy NASA Lewis Research Center).

Table 2.6 GPU-3 rhombic drive engine Ideal Isothermal simulation.

Engine and operating parameters		
Clearance volumes		$V_{clc} = 28.68$ cc
		$V_{cle} = 30.52$ cc
Swept volumes		$V_{swc} = 114.13$ cc
		$V_{swe} = 120.82$ cc
Void volumes:	Cooler	$V_k = 13.18$ cc
	Regenerator	$V_r = 50.55$ cc
	Heater	$V_h = 70.28$ cc
Mean pressure		$p_{mean} = 41.3$ bar
Mass of gas in engine		$M = 1.1362$ g
Hot space temperature		$T_h = 977$ K
Cold space temperature		$T_k = 288$ K
Ideal Isothermal performance		
Work done		$W = 177.9$ J/cycle
Heat transferred to gas in hot space		$Q_e = 252.3$ J/cycle
Heat transferred to gas in cold space		$Q_c = -74.4$ J/cycle
Thermal efficiency		$\eta = W/Q_e = 70.5\%$
Indicated power output		Power = 7442 W at 41.72 Hz

minimum volume positions α_{min} is 130°, whereas with respect to the maximum volume positions α_{max} is 110°. In figure 2.10 we have arbitrarily defined a 'pseudo phase angle advance' α as being the algebraic mean between α_{min} and α_{max}.

The total mass of gas in the system has been calculated from the mean pressure p_{mean} on the assumption that the volume variations can be simply described in terms of fundamental sinusoids. This is the most convenient way to relate the mass to the mean pressure, and the resulting pressure values in figure 2.13 show it to be reasonable.

The Ideal Isothermal power output and efficiency of 7442 W and 70.5% are seen to be about twice as high as the actual values measured of 3958 W and 35% respectively. In the following chapters we shall attempt to evaluate the various reasons for these discrepancies quantitatively.

2.6 Case study—The Ross yoke drive engine

A Rider type of Stirling engine driven by a unique yoke linkage was recently devised by Andy Ross of Colombus, Ohio. A 25 cc model of the engine using air as the working gas was built and tested by Ross and is described by Martini (1981). Using the component sizing suggested by Ross, a dual engine was built and evaluated at Ormat Turbines, Israel, and is shown in figures 2.14 and 2.15.

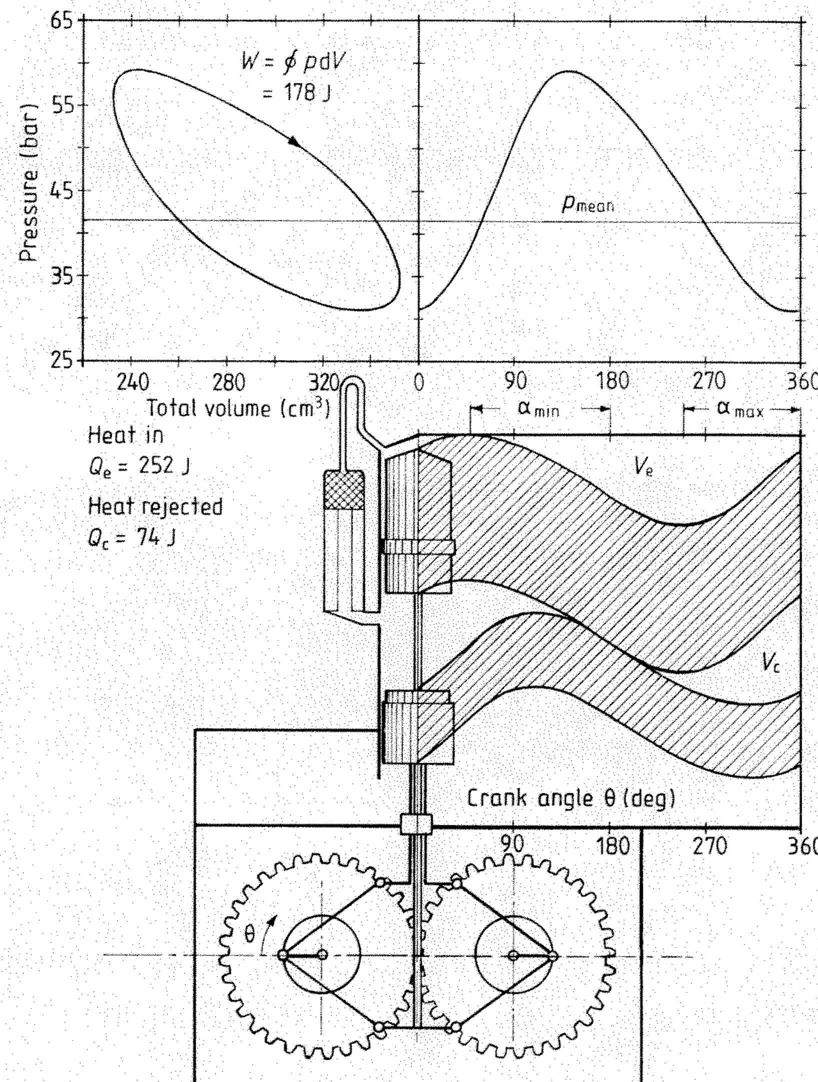

Figure 2.13 GPU-3 rhombic drive engine—Ideal Isothermal simulation.

The engine uses a conventional crank mechanism driving two pistons by means of a yoke linkage. The major feature of this is that there is almost no lateral movement of the connecting rods resulting in very small side forces on the pistons. The basic engine is very similar to the earlier Rider engine described in Chapter 1 in that it includes two working pistons on a single crank mechanism in an Alpha configuration.

With the lack of lateral movement of the connecting rods, there are relatively large unbalanced lateral forces due to the crankshaft counterweight. Ross has a patented gear mechanism which balances the lateral forces by splitting and counter-rotating the counterweights. The Ormat engine overcomes the balancing problem by directly coupling two engine units with a 180° phase difference, as shown in figure 2.15.

The engine is a demonstration model, and as such has an electrical resistance